2024-11-05

Sex-dependent additive effects of dorzagliatin and incretin on insulin secretion in a novel mouse model of *GCK*-MODY

Shadai Salazar[1–], Luis Fernando Delgadillo-Silva[1–], Priscila Carapeto[1–], Karen Dakessian[1], Rana Melhem[1], Audrey Provencher-Girard[1], Giada Ostinelli[1], Julie Turgeon[1], Imane Kaci[1], Francis Migneault[1], Mark O. Huising[2,3], Marie-Josée Hébert[1,4,5] and Guy A. Rutter [1,6,7,8*]

[1]CR-CHUM and University of Montreal, QC, Canada
[2]Department of Neurobiology, Physiology and Behavior, College of Biological Sciences, University of California, Davis, Davis, CA
[3]Department of Physiology and Membrane Biology, School of Medicine, University of California, Davis, Davis, CA
[4]Département de Microbiologie, Infectiologie et Immunologie, Faculté de Médecine, Université de Montréal, Montréal, QC, Canada
[5]Département de Médecine, Université de Montréal, Montréal, QC, Canada.
[6]Section of Cell Biology and Functional Genomics, Division of Diabetes, Endocrinology and Metabolism, Faculty of Medicine, Department of Metabolism, Digestion and Reproduction, Faculty of Medicine, Imperial College London, Hammersmith Hospital, W12 ONN London U.K.
[7]Research Institute of the McGill University Health Centre, Montreal, QC, Canada
[8]Lee Kong Chian School of Medicine, Nanyang Technological College, Singapore

Correspondence to g.rutter@imperial.ac.uk or guy.rutter@umontreal.ca

[–]Equal contributions

4043/4000 words max.

6 figures

0 tables

Abstract

Glucokinase (GK) catalyses the key regulatory step in glucose-stimulated insulin secretion. Correspondingly, hetero- and homozygous mutations in human *GCK* cause maturity-onset diabetes of the young (GCK-MODY) and permanent neonatal diabetes (PNDM), respectively. To explore the possible utility of glucokinase activators (GKA) and of glucagon–like receptor-1 (GLP-1) agonists in these diseases, we have developed a novel hypomorphic *Gck* allele in mice encoding an aberrantly spliced mRNA deleted for exons 2 and 3. In islets from homozygous knock-in ($Gck^{KI/KI}$) mice, GK immunoreactivity was reduced by >85%, and glucose-stimulated insulin secretion eliminated. Homozygous $Gck^{KI/KI}$ mice were smaller than wildtype littermates and displayed frank diabetes (fasting blood glucose >18 mmol/L; HbA1c ~12%), ketosis and nephropathy. Heterozygous $Gck^{KI/+}$ mice were glucose intolerant (HbA1c ~5.5%). Abnormal glucose-stimulated Ca^{2+} dynamics and beta cell-beta cell connectivity in $Gck^{KI/+}$ islets were completely reversed by the recently-developed GKA, dorzagliatin, which was largely inactive in homozygous $Gck^{KI/KI}$ mouse islets. The GLP-1 receptor agonist exendin-4 improved glucose tolerance in male $Gck^{KI/+}$ mice, an action potentiated by dorzagliatin, in male but not female mice. Sex-dependent additive effects of these agents were also observed on insulin secretion *in vitro*. Combined treatment with GKA and incretin may thus be useful in *GCK*-MODY or *GCK*-PNDM.

Article Highlights

a. Glucokinase deficiency can drive maturity-onset diabetes of the young (GCK-MODY; *heterozygotes*) and permanent neonatal diabetes (GCK-PNDM; *homozygotes*)

b. We describe a hypomorphic *Gck* allele where aberrant splicing in islets lowers GK activity to by ~85%. We use these mice to explore the effects of the glucokinase activator, dorzagliatin, and incretin on insulin secretion

c. Whereas heterozygous mutant mice are mildly hyperglycemic, homozygotes have frank diabetes but survive to adulthood. Dorzagliatin potentiates the effects of GLP-1 receptor activation sex-dependently in heterozygotes

d. Combined use of these drugs may be useful in some forms of *GCK* diabetes

Keywords

Glucokinase; GCK-MODY, GCK-PNDM; incretin, insulin secretion; islet; beta cell; mouse model; calcium imaging

Introduction

Diabetes affects more than 1 in 10 of the global adult population (1), a figure expected to grow to >750m people by 2045 (2). Glucokinase (Hexokinase-4, HK-IV, EC 2.7.1.1, GK) catalyses the flux-generating step in glycolysis and has been dubbed the "glucose sensor" of the pancreatic beta cell (3-7). After phosphorylation by GK, glucose carbons flow through the glycolytic pathway and enter the citrate cycle, stimulating respiratory chain activity to increase cytosolic ATP/ADP ratios. Closure of ATP-sensitive K^+ channels leads to depolarisation of the plasma membrane, Ca^{2+} influx through voltage-gated calcium channels, and insulin release (8; 9). Roles for other coupling factors (10; 11), and local ATP/ADP microdomains (12), are also proposed (13), though the latter are disputed (14).

Homozygosity for GK (*GCK)* loss-of-function (LoF) alleles results in permanent neonatal diabetes mellitus (PNDM) (15), often requiring insulin treatment shortly after birth (16-18). Heterozygosity for LoF mutations is associated with maturity onset diabetes of the young (MODY) (19; 20). *GCK*-MODY (formerly MODY2) accounts for 20-30% of all MODY cases. Although chronically hyperglycemic (fasting glucose 6-8 mM) (21), *GCK*-MODY patients are largely asymptomatic (21). However, fetal macrosomia is an important complication in pregnancy (22).

Several mouse models have been generated to explore how *Gck* insufficiency impacts whole body metabolism (23). Animals deleted for exon 2 and incorporating a frameshift mutation (24), or exon 4 plus parts of exons 3 and 5 (25), respectively show *in utero* or perinatal mortality as homozygotes, and mild hyperglycemia as heterozygotes. Beta cell-selective *Gck* knock-outs display severe hyperglycemia, and die a few days after birth (26; 27)**.** Demonstrating the importance of islet dysfunction in the impact of these mutations, rescue of *Gck* expression selectively in the beta cell of *Gck* null mice is sufficient to reverse lethality (25).

Incretin drugs including glucagon-like-1 (GLP-1) receptor agonists are now used widely in the clinic and provide a highly efficient treatment for T2D (28). Use of these agonists has not, up to now, been explored either in *GCK*-MODY or *GCK*-PNDM. In any case, incretin action on insulin secretion requires glucose metabolism (28), suggesting that the effects of these agents may be limited in the above diseases.

Dorzagliatin (29) is a latest-generation allosteric glucokinase activator (GKA), that has recently been shown to be therapeutically useful in *GCK*-MODY (30). The above findings raise the possibility that the combined use of incretins and GKA may provide additional benefits compared to the use of either agent alone.

Here, we explore this possibility in wildtype mice and in animals bearing a hypomorphic *Gck* allele that results in aberrant splicing and severe depletion of active GK protein. Residual GK activity is nevertheless sufficient to allow the survival of homozygous mice into adulthood, despite severe diabetes, modelling *GCK*-PNDM. Heterozygous $Gck^{KI/+}$ mice provide a convenient model of *GCK*-MODY. We test the potential therapeutic utility of glucokinase activators and incretins in both models.

Materials and Methods

Generation of hypomorphic *Gck* (C57BL6/J-Gck$^{tm1(mCard)/Rutt}$, Gck^{KI}) alleles.

The overall strategy, as designed with GenOway (Grenoble, Fr), is illustrated in Fig. 1A and SFig. 1. Integration of the mutant allele was confirmed by Sanger sequencing. Assessed after mRNA extraction from isolated islets of homozygous male Gck-mCardinal (*Gck*$^{KI/KI}$) mice, amplification by conventional PCR of the region from exon 1 to exon 9 of mRNA-derived cDNA from (SFig. 1B) yielded a barely-detectable band corresponding to the predicted wild-type (WT) product (~1.17kb) alongside a major product of ~850bp (~350bp less than predicted). Sanger sequencing of the latter revealed an aberrant splicing event between exons 1 and 4, eliminating the whole of exons 2 and 3 (Fig. 1B, SFig. 1C). *In silico* translation of the aberrantly-spliced isoform suggested the production of a 360 amino acids (AA) protein versus native wild type (466 AA) glucokinase. The mutant form is expected to lack amino acids 16 to 121, including residues in the small lobe encoded by exon 3, and critical for ATP binding and catalysis, e.g. R63 (6; 31; 32) .

cDNAs corresponding to the expected IRES or mCardinal regions were not detected in islets, and mCardinal fluorescence was absent from islet, liver and brain (ventromedial and lateral hypothalamus) (33) (not shown).

Animal husbandry

All experimental manipulations were approved by the local ethical committee (CRCHUM, Montreal CIPA 2022–10,040 CM21022GRs). Colonies of GK^{KI} and of GK^{KI}:Ins1Cre:GCaMP6$^{f/f}$ and GK^{KI}:Ins1Cre:GCCaMP6$^{f/f}$ mice, in which the Ca^{2+} sensor GCaMP6f is expressed selectively in the beta cell (34), on a C57BL/6J background, were fed a regular chow diet and maintained at controlled temperature (21–23 °C), humidity (45–50 %) and light (12 h day-night cycle).

Structural modelling

We compared the Alpha fold-predicted 3D protein structure against the X-ray crystal-resolved human Glucokinase (3VEY, www.rcsb.org/structure/3VEY). Additionally, we compared the previously AI-generated model of mouse Glucokinase (35). The 3D comparison was generated by PDB Mol View (Pairwise Structure Alignment

https://www.rcsb.org/alignment) using the TM-algin method. The TM-align method is based on structure comparison for proteins with similar global topology. ClustalW was employed to quantify amino acid sequence similarity.

Intraperitoneal glucose tolerance tests (IPGTT)

Mice were fasted overnight (16 h) with free access to water. At 9 am, glucose (2 g/kg body weight) was administered *via* intraperitoneal injection. Blood glucose levels were measured from the tail vein 0, 15, 30, 60 and 90 min. later with an automatic glucometer (Contour next ONE; Canada) (36).

Insulin tolerance tests

After 6 h fasting with free access to water, human insulin (Novolin-ge Toronto, Novo Nordisk) (1 U/kg body weight) was administered *via* intraperitoneal injection. Blood glucose was measured as above (36).

Islet isolation.

Islets were isolated from mice aged between 8 and 16 weeks, essentially as previously described (37).

Measurement of insulin secretion *in vitro*

Initially, insulin secretion was assessed using the following buffer, containing (mmol/L) 137 NaCl, 4.8 KCl, 1.2 KH_2PO_4, 1.2 $MgSO_4$, 2.5 $CaCl_2$·2H2O, 5 $NaHCO_3$, and 16 HEPES, adjusted to pH 7.4 and supplemented with 0.1% BSA. Islets were pre-incubated in low glucose (3 mM) for 1 h, the sequentially for 1 h at 3 mmol/L then 17 mmol/L glucose (see Fig. 3, H,I). In experiments involving agonist treatment (Fig. 6), isolated islets were incubated in modified KRBH stock solutions comprising (mmol/L) 10 HEPES, 2 $NaHCO_3$, 137 NaCl, 3.6 KCl, 0.5 NaH_2PO4, 0.5 MgSO4, 1.5 $CaCl_2$. Solutions were gassed with 95% O_2 and 5% CO_2 and adjusted to pH 7.4. The buffer was maintained at 37°C and supplemented with 0.1% BSA. Islets were selected based on size, washed, and incubated in KRBH-BSA with 3 mmol/L glucose for 1 h then transferred to 12-well plates and divided into four groups, each in triplicate: (1) control (2) plus Dorzagliatin (10 µM), (3) Exendin-4 (100 nmol/L), (4) Dorzagliatin and Exendin-4. Islets were incubated for 30 min. in low glucose (3 mmol/L), then at high (17 mmol/L) glucose. All samples

were stored at -80°C until measurement using an Insulin Ultrasensitive HTRF Assay Kit (Revvity, 62IN2PEG).

Beta- and alpha-cell mass

After transcardiac perfusion, the pancreas was carefully dissected, weighed, and placed in cassettes for fixation in 4%(v/v) paraformaldehyde (PFA) for 2h to facilitate paraffin embedding. Adjacent full footprint sections were then subjected to immunostaining for glucagon (Cell Signaling, 2760) or insulin (Cell Signaling, 4590) using a standard DAB substrate kit (Cell Signaling, 8059). Incubations with primary antibodies were performed overnight at 4°C, at an antibody dilution of 1:100. The mass of β-cells and α-cells was quantified using point counting morphometry (38).

Renal histology

Whole kidney was dissected after transcardiac perfusion and fixed in 4%(v/v) PFA for an extra 2 h, then paraffin-embedded. Histology analysis was done at a 20x magnification, on whole kidney sections. Images were taken with Slide Scanner Leica, Aperio Versa 200 digital scanner and further analyzed in the Aperio ImageScope 12.43.3 software. Renal tubular damage was described based on luminal dilatation and necrosis, loss of brush border, and cast formation. The investigator was blinded to experimental conditions.

PCR and qPCR

Specific primers for *Glucokinase* cDNA amplification from exon 1 to the mCardinal sequence are reported in Supp. Table 1. Briefly, was cDNA synthesized from total Trizol-Chloroform purified mRNA from isolated islets of either $Gck^{KI/KI}$ or WT animals. cDNA was synthesized using High-Capacity cDNA Reverse Transcription kit (Applied biosystems, Thermo-Fisher). After PCR amplification of exon 1 and exon 9, the product was migrated on a 1.0% agarose gel, the ~850bp band was excised, purified and Sanger sequenced (Genome-Quebec, Canada).

Calcium imaging

Ca^{2+} imaging was performed essentially as described (39; 40) using a Zeiss LSM 900 Airyscan 2 super-resolution confocal microscope, equipped with an incubation system set at 37°C. A 40×/1.3 Apochromat oil immersion objective was employed with a frame

rate of 150ms (~6Hz) with 512 x 512 px image size. 1h before imaging, islets were transferred into Krebs buffer (130 mM NaCl, 3.6 mM KCl, 1.5 mM $CaCl_2$, 0.5 mM $MgSO_4$, 0.5 mM NaH_2PO_4, 24 mM $NaHCO_3$, 10 mM HEPES; pH 7.4), containing 3 mmol/L glucose. For Dorzagliatin (HMS5552; Abmol Biosciences) (41; 42) treatment, islets were transferred to Krebs buffer with 1% DMSO and 10 µm Dorzagliatin for 1h prior to imaging. Imaging was performed at 11 mM glucose.

Connectivity analysis

Analysis was performed essentially as per (39), with modifications. Fluorescence traces were normalized using the formula:

$$(F_T – F_{MIN}) / F_{MIN}$$

Smoothing was used to adjust Ca^{2+} signals via a moving average filter, contributing to 1% of the total length of the Ca^{2+} recording. Cell activity was represented in binary form, where any time point deviating >20% above the baseline was considered to be active, represented by “1”. Any inactive time point, under the threshold, is represented by a “0”. The following formula was used to calculate coactivity for each cell pair:

$$Cij=Tij-sqr(Ti*Tj)$$

Tij denotes the total coactivity of each cell pair. *Ti* and *Tj* are the total activity time for the two cells compared, respectively.

Cells are considered to be linked if their t-test displayed a chance (>2 standard deviations i.e. $p<0.01$) probability within a corresponding distribution of the shuffled (10,000 times) binarized observed dataset, for the analyzed cell pairs.

A topographic representation of the connectivity was plotted in MATLAB (available from: https:--www.mathworks.com-matlabcentral-fileexchange-24035-wgplot-weighted-graph-plot-a-better-version-of-gplot). Edge colors indicate the strength of the coactivity. Highly connected (“Hub”) cells were defined as those where >70 % of connections had a connectivity value of >0.7.

Western (immuno-) blotting

Blotting was performed *as per* (43). Isolated islets were washed twice with PBS, and fast frozen on dry ice. To extract proteins, 10uL of RIPA buffer plus protease inhibitors was added to 100 islets, and samples sonicated for 3s on ice. Protein concentration was estimated by Pierce BCA protein assay (ThermoFisher). One volume of Laemmli (4x) solubilization buffer was added, followed by exposure to 95□C for 60s to denature proteins. 10µg protein per lane was loaded onto 10%(w/v) acrylamide gels. For liver, lung and heart, 10uL RIPA buffer with protease inhibitors per mg wet weight was added. Protein extract (20µg) was loaded onto each lane. After electrophoresis, proteins were transferred to PVDF membranes. Membranes were blocked with 3% BSA, TBST 1%. After 1h, membranes were incubated with primary antibody overnight at 4□C. Membranes were washed with TBST 1% before incubation with secondary antibody (1h, room temperature). Horseradish peroxidase (HRP) chemiluminescent substrate (ECL western substrate, Thermo) was used to reveal bound antibody.

Statistics

Data are expressed as mean ± SD, unless otherwise stated and significance tested by one or two-way ANOVA with Šidák or Brown-Forsythe multiple comparison tests, using GraphPad Prism 9 (GraphPad Software, San Diego, CA). $P < 0.05$ was considered significant.

Data resource and availability

All data generated or analyzed during this study are included in the published article (and its online supplementary files. Details of movies are provided in the Supp. Figure document, which includes original gel blots in SFig.s 8,9). Analytical scripts are provided at https://zenodo.org/records/14042795.

Results.

Generation of a hypomorphic *Gck* allele

With the initial objective of identifying beta cell subpopulations enriched for GK (which may correspond to highly connected "hub" cells) (44), we designed a "knock-in" construct encoding exons 3-10 of mouse *Gck*, followed by an internal ribosome entry site (IRES), cDNA encoding the fluorescent protein mCardinal, and a polyA sequence (Materials and Methods, Fig. 1A,C, SFig. 1A). Genomic sequencing confirmed the expected integration at the *Gck* locus (not shown). However, and unexpectedly, an alternatively-spliced product was generated, predicted to encode a mutant protein that lacks much of the small lobe of GK (31).

GK protein levels in islets from wild type and mutant mice were assessed by Western (immuno-) blotting (Fig. 2). *Gck* is expressed from different promoters in the liver and in the pancreatic beta cell (45). Consequently, the first 15 amino acids (AAs) encoded by exon 1 from the beta cell promoter differ from those of the equivalent exon encoded in the liver (6). The antibody deployed (Thermofisher Glucokinase Antibody PA5-15072) is raised against the first 30 AA of type 1 GK (islet). Loss of the following 16 AA (encoded by exon 2) from the epitope is thus likely to weaken or destroy recognition by the antibody of the mis-spliced isoform. This approach revealed a 30-45% and $\geq$85% lowering in apparent GK immunoreactivity (~48 kDa) in islets from $GK^{KI/+}$ and $GK^{KI/KI}$ islets, respectively, *versus* control mice of either sex, indicating a proportionate lowering of the intact isoform 1 protein (including exons 2 and 3) (Figure 2B). We note that, if present, the mutant is expected to be inactive, given (a) the requirement for the ATP binding sites encoded by exon 3 (6) and (b) the likely absence, based on structural prediction with AlphaFold (see Methods, Fig. 1D,E, S.Movie1), of a properly-folded glucose-binding beta sheet in the small lobe.

No differences in immunoreactivity at this molecular weight were observed in liver extracts from WT, $Gck^{KI/+}$ and $Gck^{KI/KI}$ animals, presumably reflecting the failure of the antibody to recognise the liver isoform (SFig. 2).

Metabolic characterisation of *Gck* mutant mice

Examined at 8 weeks of age, heterozygous ($Gck^{KI/+}$) mice displayed normal body weight, whilst male homozygous ($Gck^{KI/KI}$) animals were lighter than littermate controls (Fig.

3A,B); a similar tendency was seen in females (Fig. 3B). HbA1c levels tended to be elevated, or were drastically increased, respectively, in $Gck^{KI/+}$ and $Gck^{KI/KI}$ animals *versus* controls (Fig. 3C). Fasting blood glucose (FBG) was >18 mmol/L in the latter animals of either sex at eight weeks of age (males, *n*=7, 21.6 to>33.3 mmol/L; females, *n*=5, 18.4-27.4 mmol/L; Fig. 3D,F). Whereas overnight (16 h) FBG did not differ between $Gck^{+/+}$ and $Gck^{KI/+}$ mice of either sex (Fig. 3D,E), $Gck^{KI/+}$ animals displayed markedly abnormal glucose tolerance, with no return to pre-infusion levels after 90 min. Blood glucose levels after 6 h fasting were higher in $Gck^{KI/+}$ *versus* WT mice (Fig. 3F,G,). Insulin sensitivity did not differ between genotypes, after correction for FBG (Fig. 3F *insets*, Fig. 3G).

Measured in batch incubations, glucose-stimulated insulin secretion (GSIS) from male islets was lowered by ~50 % in $Gck^{KI/+}$ versus controls, and eliminated in homozygous $Gck^{KI/KI}$ islets (Fig. 3H). In females, GSIS was unaffected in $Gck^{KI/+}$ but eliminated in $Gck^{KI/KI}$ islets (Fig. 3H).

Whilst also unaltered in $Gck^{KI/+}$ mice *versus* controls, beta cell mass was substantially (~65% in males, ~50 % in females) lowered in $Gck^{KI/KI}$ animals (SFig. 3). Conversely, alpha cell numbers were markedly increased in $Gck^{KI/KI}$ mice (~2-fold in both sexes; SFig. 3). Consequently, the beta:alpha cell ratio fell from ~10:1.0 in wildtype to ~1.0:1.0 in $Gck^{KI/KI}$ pancreata.

Consistent with frank diabetes, ketone levels tended to be, or were significantly, increased in male and female $Gck^{KI/KI}$ animals *versus* controls, respectively (Fig. 3I). Moreover, in the kidney, homozygous $Gck^{KI/KI}$ mice of either sex displayed clear tubular alterations compared to heterozygous $Gck^{KI/+}$ and control mice (SFig. 4; Supp. Table 2).

Ca^{2+} dynamics and intercellular connectivity

The above findings suggested that defects may exist in intracellular glucose handling or signalling in mutant beta cells. To explore this possibility, we studied glucose-regulated intracellular Ca^{2+} dynamics and cell-cell connectivity in isolated islets using high speed confocal imaging (Fig.4A) (44). To ensure that Ca^{2+} was measured exclusively in beta cells, mice were bred to animals carrying Ins1*Cre* alleles (46) and STOP-Flox alleles of the genetic Ca^{2+} sensor, GCaMP6f (34). Male animals carrying wild type *Gck* alleles displayed robust responses to stimulation with 11 mM glucose, and a high degree of connectivity (Fig. 4B-E; SMovie 2,3). These responses were significantly weakened in

$Gck^{KI/+}$ mice and almost completely eliminated in $Gck^{KI/KI}$ animals. Similar behaviour was seen in islets from animals of both sexes, though the Ca^{2+} responses (area under the curve, AUC) were lower in females than males (Fig. 4, E-G SFig. 6). Remarkably, these responses were fully normalized with dorzagliatin in $Gck^{KI/+}$ mice of both sexes Fig.4F,G, SFig. 6, SMovie 4,5), but barely affected in $Gck^{KI/KI}$ mice. Nevertheless, a subset of female $Gck^{KI/KI}$ islets showed detectable Ca^{2+} transients in response to glucose stimulation in the presence of dorzagliatin (Fig. 4, F,G).

Responses of wildtype and $Gck^{KI/+}$ mice to GKA and incretin *in vivo*.

Given the findings above, we next explored the effects of dorzagliatin *in vivo* during intraperitoneal glucose tolerance tests (IPGTT), in the presence or absence of the GLP-1 receptor agonist, exendin-4.

Examined in wildtype mice of either sex, acute injection of dorzagliatin or exendin-4 alone exerted only minor effects on glucose tolerance, which did not reach statistical significance (Fig. 5A-D). On the other hand, in wildtype male (but not female) mice, co-injection of dorzagliatin markedly potentiated the action of exendin-4 (Fig. 5A-D).

In male heterozygous $Gck^{KI/+}$ mice, exendin-4 alone, but not dorzagliatin, improved glucose tolerance, whilst the combination of exendin-4 and dorzagliatin profoundly lowered glucose excursions to levels comparable to those in wildtype mice (Fig. 5, A,C). In female $Gck^{KI/+}$ mice, dorzagliatin again exerted no effect when administered alone, whereas exendin-4 markedly improved glucose tolerance. No additional effect was observed of co-injecting dorzagliatin and exendin-4 (Fig. 5 B,D).

Combining data from both sexes, we noted that neither drug, alone or in combination, significantly affected glycemia in homozygous ($Gck^{KI/KI}$) animals (Fig.5E).

Effects of incretin and GKA on glucose-stimulated insulin secretion

Explored *in vivo* during IPGTTs, glucose-induced increases in circulating insulin tended to be potentiated by incretin in male, but not female, $Gck^{+/+}$ and $Gck^{KI/+}$ mice (SFig. 6). Since inter-animal variation was large in these experiments, we examined the potential interaction between the GKA and incretin on insulin secretion *ex vivo*. In islets isolated from wildtype male mice, neither dorzagliatin nor exendin-4 significantly affected insulin secretion stimulated by 17 mmol/L glucose (Fig. 6A). In contrast, the combination of dorzagliatin and exendin-4 stimulated hormone release 2.0-2.5-fold. In islets from male

$Gck^{KI/+}$ mice (Fig. 6A), dorzagliatin alone tended to increase secretion, whilst exendin-4 alone caused a ~3-fold increase in hormone release. The effect of incretin was further augmented by dorzagliatin (~5-fold increase *versus* 17 mmol/L glucose alone). Qualitatively similar results were obtained in female wildtype mice (Fig. 6B). In female $Gck^{KI/+}$ islets, the effects of dorzagliatin or exendin-4, whether administered alone or together, were weaker than those in $Gck^{KI/+}$ males (Fig. 6B *versus* Fig.6A).

When data from both sexes were pooled, exendin-4 was found to potentiate glucose-stimulated insulin secretion in $Gck^{KI/+}$ islets, an action further enhanced by dorzagliatin (Fig. 6C). Similar, albeit nonsignificant, tendencies were observed in wildtype and in $Gck^{KI/KI}$ islets (Fig. 6C).

Discussion.

Novel models of "glucokinase" diabetes.

We describe here novel mouse models of *GCK*-MODY and *GCK*-PNDM, and explore the potentiation of glucose-stimulated insulin secretion by a glucokinase activator and incretin in each case.

More than 600 variants are associated with human *GCK*-MODY, with eight identified in *GCK*-PNDM (47). The latter vary in their effects on GK activity or stability, and have broadly proportional clinical impacts (21). Whilst homozygosity for mutants with near-zero activity is usually implicated in PNDM, compound heterozygosity for an inactivating (e.g. (intervening sequence 8 [IVS8] + 2T→G) and hypomorphic (G264S) variant (16) can also drive neonatal diabetes. On the other hand, milder mutations e.g. G223S, L315H, with relative activities of 0.25 and 0.89, respectively (48), lead to *GCK*-MODY. Interestingly in the context of the present study, Osbak *et al* have speculated that milder *GCK* mutations in *GCK*-PNDM e.g. R397L (16; 49) may be more responsive to GKA than those leading to more complete inactivation e.g, T168A (50).

The hypomorphic *Gck* allele described here was originally designed to preserve an intact glucokinase protein, whilst independently expressing, from the same transcript, the fluorescent reporter mCardinal. Instead, an unexpected splicing event eliminated exons 2 and 3 (encoded by the host genome) and led to the fusion of exon 1 to exon 4, derived from the introduced *Gck* cDNA (exons 4-11). The aberrantly-spliced transcript is predicted to produce an inactive protein, lacking much of the ATP- and glucose-binding catalytic domain of the smaller lobe (31). It is also possible that the variant transcript fails to produce any protein product at all. Our Western blotting approach was unable to distinguish between these possibilities, since the product of the aberrantly-spliced variant is unlikely to be detected by the N-terminal targeting antibody used (Results).

In any case, limited correct splicing appears to produce low levels of the active, wildtype protein (10-15% of normal values). Consequently, the Gck^{KI} allele provides a convenient model of inactivating *GCK* mutations that affect the kinetic properties of GK as well as of variants that lead to thermal instability and protein degradation (51).

Enzymatic measurements of GK were not performed since these require beta cell purification to exclude contamination from hexokinases I-III abundant in other cell types (52). Nevertheless, the metabolic features of homozygous *Gck*$^{KI/Ki}$ mice (Fig. 3,5), studies of glucose regulated Ca^{2+} dynamics (Fig. 4; SFig 5) and insulin secretion (Fig.s 3,6) are consistent with near-complete elimination of GK activity from the beta (and other pancreatic endocrine) cells. The persistence of residual glucokinase activity in beta cells likely explains why homozygous Gck$^{KI/KI}$ mice survive into adulthood, in contrast with models of complete *Gck* inactivation (23) (see Introduction). Of note, the metabolic phenotype of heterozygous (Gck$^{KI/+}$) mice was almost indistinguishable from that of previous models involving complete inactivation of a single allele, and thus is compatible with loss of 40-45% of GK activity. Ca^{2+} imaging revealed the expected defects in glucose signaling in both Gck$^{KI/+}$ and Gck$^{KI/KI}$ islets, and the expected rescue of these deficits by dorzagliatin in the former, reflecting the activation of the remaining glucokinase. Whilst the glucokinase activator was largely inactive in male Gck$^{KI/KI}$ islets, as anticipated, 10-30 % of islets displayed responses to dorzagliatin in females (Fig. 4F,G). Interestingly, these findings suggest that correctly spliced, active, GK may be restricted to a subset of Gck$^{KI/KI}$ islets.

Our observation of lowered beta cell mass in homozygous mice aligns with earlier studies in glucokinase-deficient mice (53). Less expected was the increase in alpha cell mass in Gck$^{KI/KI}$ islets, suggesting that GK activity plays a role in suppressing alpha cell expansion, in addition to inhibiting glucagon secretion (54). Extrapolated to humans, these findings raise the intriguing possibility that elevated glucagon levels may aggravate hyperglycemia in *GCK*-PNDM.

We note that, in addition to islets and liver, glucokinase is expressed in several brain nuclei, including the hypothalamus, pituitary and brain stem (33), as well as in intestinal L-cells (55). As such, the phenotypes of Gck$^{KI/+}$ and Gck$^{KI/KI}$ mice may in part reflect actions on these cell types.

Sex-dependent additive effects of dorzagliatin and incretin on glucose tolerance and insulin secretion.

Previous work with earlier-generation GKAs (e.g. the AstraZeneca molecule, GKA50) (56), reported a marked left-shift in the response to glucose in both mouse and human islets. Under the conditions used here, involving high glucose concentrations in both

settings, dorzagliatin alone elicited minimal effects either *in vivo* on glucose tolerance (Fig 5 C,D,E), or on glucose-stimulated insulin secretion (Fig. 6A,B) both in wildtype and $Gck^{KI/+}$ mice. Nevertheless, the GKA markedly potentiated the effects of exendin-4 on glucose-stimulated insulin secretion both *in vivo* (Fig. 5C) and *in vitro* (Fig. 6A), an effect most dramatic in heterozygous male mice. The mechanisms underlying this apparent sexual dimorphism in drug responses remain unclear.

Conclusions. We describe here new mouse models of *GCK*-MODY and *GCK*-PNDM, which may be valuable for future drug screens as well as studies of diabetes complications, including nephropathy. We demonstrate the remarkable efficacy in the former of combining a GKA with a GLP-1R agonist, likely reflecting a requirement for beta cell glucose metabolism for incretin action (28). Our findings suggest the potential therapeutic utility of this drug combination in selected *GCK*-MODY or *GCK*-PNDM patients.

Acknowledgements

We thank the CRCHUM Cell Imaging, Animal and Cellular Physiology Facilities for their assistance and Jannick Bonenfant (UdeM) for help with imaging experiments. We are grateful to Drs Khalil Boudaydan, Demetra Rodaros and Thierry Alquier (CRCHUM) for fluorescence measurements in liver and brain sections.

Funding

G.A.R. was supported by a Wellcome Trust Investigator Award (WT212625/Z/18/Z), MRC Programme grant (MR/R022259/1), Diabetes UK (BDA 16/0005485) and NIH-NIDDK (R01DK135268) project grants, a CIHR-JDRF Team grant (CIHR-IRSC TDP-186358 and JDRF 4-SRA-2023-1182-S-N), CRCHUM start-up funds, and an Innovation Canada John R. Evans Leader Award (CFI 42649). LD was support by a CIHR/IRSC Post-doctoral Fellowship (#489982), PC and GO by Fonds de Recherche du Quebec, Nature and Technology Fellowships (#353239, #333916).

Duality of Interest. G.A.R. has received grant funding from, and is a consultant for, Sun Pharmaceuticals Inc. No other potential conflicts of interest relevant to this article were reported.

Author contributions

GAR and MOH conceived the project. GAR designed the studies, supervised the project and wrote the manuscript with input from all authors. SS and LD performed *in vivo* metabolic analyses, and studies of Ca^{2+} dynamics, alongside GO and KD. KB, DR, WT and TA performed histological studies and immunohistochemistry of liver and brain sections. IK, JT, FM and MJH analysed kidney sections with PC, who performed *in vitro* insulin secretion analyses with RM and quantified beta/alpha cell mass. LD, KD, RM and SS performed analysis of alternative splicing, and LD structural modelling with AlphaFold.

G.A.R. serves as guarantor of the study.

REFERENCES

1. International Diabetes Federation: https://idf.org/news/diabetes-now-affects-one-in-10-adults-worldwide/. 2023;
2. Saeedi P, Petersohn I, Salpea P, Malanda B, Karuranga S, Unwin N, Colagiuri S, Guariguata L, Motala AA, Ogurtsova K, Shaw JE, Bright D, Williams R: Global and regional diabetes prevalence estimates for 2019 and projections for 2030 and 2045: Results from the International Diabetes Federation Diabetes Atlas, 9(th) edition. Diabetes Res Clin Pract 2019;157:107843
3. Coore HG, Randle PJ: Inhibition of glucose phosphorylation by mannoheptulose. Biochemical Journal 1964;91:56-59
4. Grodsky GM, Batts AA, Bennett LL, Vcella C, McWilliams NB, Smith DF: Effects of carbohydrates on secretion of insulin from isolated rat pancreas. Am J Physiol 1963;205:638-644
5. Meglasson MD, Matschinsky FM: Pancreatic islet glucose metabolism and regulation of insulin secretion. Diabetes/Metabolism Reviews 1986;2:163-214
6. Iynedjian PB: Mammalian glucokinase and its gene. BiochemJ 1993;293:1-13
7. Matschinsky FM: Banting Lecture 1995. A lesson in metabolic regulation inspired by the glucokinase glucose sensor paradigm. Diabetes 1996;45:223-241
8. Rorsman P, Ashcroft FM: Pancreatic beta-Cell Electrical Activity and Insulin Secretion: Of Mice and Men. Physiol Rev 2018;98:117-214
9. Rutter GA, Sidarala V, Kaufman BA, Soleimanpour SA: Mitochondrial metabolism and dynamics in pancreatic beta cell glucose sensing. Biochem J 2023;480:773-789
10. Henquin JC: Regulation of insulin secretion: a matter of phase control and amplitude modulation. Diabetologia 2009;52:739-751
11. Prentki M, Madiraju SR: Glycerolipid/free fatty acid cycle and islet beta-cell function in health, obesity and diabetes. MolCell Endocrinol 2012;353:88-100
12. Kennedy HJ, Pouli AE, Ainscow EK, Jouaville LS, Rizzuto R, Rutter GA: Glucose generates sub-plasma membrane ATP microdomains in single islet beta-cells. Potential role for strategically located mitochondria. J Biol Chem 1999;274:13281-13291
13. Foster HR, Ho T, Potapenko E, Sdao SM, Huang SM, Lewandowski SL, VanDeusen HR, Davidson SM, Cardone RL, Prentki M, Kibbey RG, Merrins MJ: β-cell deletion of the PKm1 and PKm2 isoforms of pyruvate kinase in mice reveals their essential role as nutrient sensors for the K(ATP) channel. Elife 2022;11
14. Rutter GA, Sweet IR: Glucose Regulation of β-Cell KATP Channels: Is a New Model Needed? Diabetes 2024;73:849-855
15. De León DD, Stanley CA: Permanent Neonatal Diabetes Mellitus. In *GeneReviews(®)* Adam MP, Feldman J, Mirzaa GM, Pagon RA, Wallace SE, Amemiya A, Eds. Seattle (WA), University of Washington, SeattleCopyright © 1993-2024, University of Washington, Seattle. GeneReviews is a registered trademark of the University of Washington, Seattle. All rights reserved., 1993

16. Njølstad PR, Sagen JV, Bjørkhaug L, Odili S, Shehadeh N, Bakry D, Sarici SU, Alpay F, Molnes J, Molven A, Søvik O, Matschinsky FM: Permanent neonatal diabetes caused by glucokinase deficiency: inborn error of the glucose-insulin signaling pathway. Diabetes 2003;52:2854-2860
17. Njølstad PR, Søvik O, Cuesta-Muñoz A, Bjørkhaug L, Massa O, Barbetti F, Undlien DE, Shiota C, Magnuson MA, Molven A, Matschinsky FM, Bell GI: Neonatal diabetes mellitus due to complete glucokinase deficiency. N Engl J Med 2001;344:1588-1592
18. Durmaz E, Flanagan S, Berdeli A, Semiz S, Akcurin S, Ellard S, Bircan I: Variability in the age at diagnosis of diabetes in two unrelated patients with a homozygous glucokinase gene mutation. J Pediatr Endocrinol Metab 2012;25:805-808

19. Vionnet N, Stoffel M, Takeda J, Yasuda K, Bell GI, Zouali H, Lesage S, Velho G, Iris F, Passa P: Nonsense mutation in the glucokinase gene causes early-onset non-insulin-dependent diabetes mellitus. Nature 1992;356:721-722
20. Stoffel M, Patel P, Lo YM, Hattersley AT, Lucassen AM, Page R, Bell JI, Bell GI, Turner RC, Wainscoat JS: Missense glucokinase mutation in maturity-onset diabetes of the young and mutation screening in late-onset diabetes. Nat Genet 1992;2:153-156
21. Gersing S, Cagiada M, Gebbia M, Gjesing AP, Coté AG, Seesankar G, Li R, Tabet D, Weile J, Stein A, Gloyn AL, Hansen T, Roth FP, Lindorff-Larsen K, Hartmann-Petersen R: A comprehensive map of human glucokinase variant activity. Genome Biol 2023;24:97
22. Kirzhner A, Barak O, Vaisbuch E, Zornitzki T, Schiller T: The Challenges of Treating Glucokinase MODY during Pregnancy: A Review of Maternal and Fetal Outcomes. Int J Environ Res Public Health 2022;19
23. Abu Aqel Y, Alnesf A, Aigha II, Islam Z, Kolatkar PR, Teo A, Abdelalim EM: Glucokinase (GCK) in diabetes: from molecular mechanisms to disease pathogenesis. Cell Mol Biol Lett 2024;29:120
24. Bali D, Svetlanov A, Lee HW, FuscoDeMane D, Leiser M, Li B, Barzilai N, Surana M, Hou H, Fleischer N, DePinho R, Rossetti L, Efrat SNADMPAECM: Animal model for maturity-onset diabetes of the young generated by disruption of the mouse glucokinase gene. Journal of Biological Chemistry 1995;270:21464-21467
25. Grupe A, Hultgren B, Ryan A, Yan Hui M, Bauer M, Stewart TA: Transgenic knockouts reveal a critical requirement for pancreatic beta cell glucokinase in maintaining glucose homeostasis. Cell 1995;83:69-78
26. Postic C, Shiota M, Niswender KD, Jetton TL, Chen Y, Moates JM, Shelton KD, Lindner J, Cherrington AD, Magnuson MA: Dual roles for glucokinase in glucose homeostasis as determined by liver and pancreatic beta cell-specific gene knock-outs using Cre recombinase. JBiolChem 1999;274:305-315
27. Terauchi Y, Sakura H, Yasuda K, Iwamoto K, Takahashi N, Ito K, Kasai H, Suzuki H, Ueda O, Kamada N, et al.: Pancreatic beta-cell-specific targeted disruption of glucokinase gene. Diabetes mellitus due to defective insulin secretion to glucose. J Biol Chem 1995;270:30253-30256
28. Nauck MA, Müller TD: Incretin hormones and type 2 diabetes. Diabetologia 2023;66:1780-1795
29. Haddad D, Dsouza VS, Al-Mulla F, Al Madhoun A: New-Generation Glucokinase Activators: Potential Game-Changers in Type 2 Diabetes Treatment. Int J Mol Sci 2024;25
30. Chow E, Wang K, Lim CKP, Tsoi STF, Fan B, Poon E, Luk AOY, Ma RCW, Ferrannini E, Mari A, Chen L, Chan JCN: Dorzagliatin, a Dual-Acting Glucokinase Activator, Increases Insulin Secretion and Glucose Sensitivity in Glucokinase Maturity-Onset Diabetes of the Young and Recent-Onset Type 2 Diabetes. Diabetes 2023;72:299-308
31. Kamata K, Mitsuya M, Nishimura T, Eiki J, Nagata Y: Structural basis for allosteric regulation of the monomeric allosteric enzyme human glucokinase. Structure 2004;12:429-438
32. Liu S, Ammirati MJ, Song X, Knafels JD, Zhang J, Greasley SE, Pfefferkorn JA, Qiu X: Insights into mechanism of glucokinase activation: observation of multiple distinct protein conformations. J Biol Chem 2012;287:13598-13610
33. Lynch RM, Tompkins LS, Brooks HL, Dunn-Meynell AA, Levin BE: Localization of glucokinase gene expression in the rat brain. Diabetes 2000;49:693-700
34. Salem V, Silva LS, Suba S, Georgiadou E, Mousavy Gharavy SN, khtar N, artin-Alonso A, aboriau DCA, othery SM, tylianides T, arrat G, Pullen TJ, Singh SP, Hodson DJ, Leclerc I, Shapiro AMJ, Marchetti P, Briant LJB, Disatso W, Ninov N, Rutter GA: Leader beta cells coordinate Ca2+ dynamics across pancreatic islets in vivo. Nat Metab 2019;1:615-629

35. Steinegger M, Söding J: Clustering huge protein sequence sets in linear time. Nat Commun 2018;9:2542
36. Akalestou E, Suba K, Lopez-Noriega L, Georgiadou E, Chabosseau P, Gallie A, Wretlind A, Quigley C, Leclerc I, Salem V, Rutter GA: Intravital imaging of islet Ca(2+) dynamics reveals enhanced ×ý cell connectivity after bariatric surgery in mice. Nat Commun 2021;12:5165
37. Ravier MA, Rutter GA: Isolation and culture of mouse pancreatic islets for ex vivo imaging studies with trappable or recombinant fluorescent probes. Methods MolBiol 2010;633:171-184
38. Montaña E, Bonner-Weir S, Weir GC: Beta cell mass and growth after syngeneic islet cell transplantation in normal and streptozocin diabetic C57BL/6 mice. J Clin Invest 1993;91:780-787
39. Chabosseau P, Yong F, Delgadillo-Silva LF, Lee EY, Melhem R, Li S, Gandhi N, Wastin J, Noriega LL, Leclerc I, Ali Y, Hughes JW, Sladek R, Martinez-Sanchez A, Rutter GA: Molecular phenotyping of single pancreatic islet leader beta cells by "Flash-Seq". Life Sci 2023;316:121436
40. Delgadillo-Silva LF, Tasöz E, Singh SP, Chawla P, Georgiadou E, Gompf A, Rutter GA, Ninov N: Optogenetic β cell interrogation in vivo reveals a functional hierarchy directing the Ca(2+) response to glucose supported by vitamin B6. Sci Adv 2024;10:eado4513
41. Xu H, Sheng L, Chen W, Yuan F, Yang M, Li H, Li X, Choi J, Zhao G, Hu T, Li Y, Zhang Y, Chen L: Safety, tolerability, pharmacokinetics, and pharmacodynamics of novel glucokinase activator HMS5552: results from a first-in-human single ascending dose study. Drug Des Devel Ther 2016;10:1619-1626
42. Wang P, Liu H, Chen L, Duan Y, Chen Q, Xi S: Effects of a Novel Glucokinase Activator, HMS5552, on Glucose Metabolism in a Rat Model of Type 2 Diabetes Mellitus. J Diabetes Res 2017;2017:5812607
43. Georgiadou E, Muralidharan C, Martinez M, Chabosseau P, Akalestou E, Tomas A, Wern FYS, Stylianides T, Wretlind A, Legido-Quigley C, Jones B, Lopez-Noriega L, Xu Y, Gu G, Alsabeeh N, Cruciani-Guglielmacci C, Magnan C, Ibberson M, Leclerc I, Ali Y, Soleimanpour SA, Linnemann AK, Rodriguez TA, Rutter GA: Mitofusins Mfn1 and Mfn2 Are Required to Preserve Glucose- but Not Incretin-Stimulated β-Cell Connectivity and Insulin Secretion. Diabetes 2022;71:1472-1489
44. Johnston NR, Mitchell RK, Haythorne E, Pessoa MP, Semplici F, Ferrer J, Piemonti L, Marchetti P, Bugliani M, Bosco D, Berishvilli E, Duncanson P, Watkinson M, Broichhagen J, Trauner D, Rutter GA, Hodson DJ: Beta cell hubs dictate pancreatic islet responses to glucose. Cell Metabolism 2016;24:389-401
45. Magnuson MA, Shelton KD: An alternate promoter in the glucokinase gene is active in the pancreatic beta cell. J Biol Chem 1989;264:15936-15942
46. Thorens B, Tarussio D, Maestro MA, Rovira M, Heikkila E, Ferrer J: Ins1 knock-in mice for beta cell-specific gene recombination. Diabetologia 2015;58:558-656
47. Osbak KK, Colclough K, Saint-Martin C, Beer NL, Bellanné-Chantelot C, Ellard S, Gloyn AL: Update on mutations in glucokinase (GCK), which cause maturity-onset diabetes of the young, permanent neonatal diabetes, and hyperinsulinemic hypoglycemia. Hum Mutat 2009;30:1512-1526
48. Valentínová L, Beer NL, Staník J, Tribble ND, van de Bunt M, Hučková M, Barrett A, Klimeš I, Gašperíková D, Gloyn AL: Identification and functional characterisation of novel glucokinase mutations causing maturity-onset diabetes of the young in Slovakia. PLoS One 2012;7:e34541
49. García-Herrero CM, Galán M, Vincent O, Flández B, Gargallo M, Delgado-Alvarez E, Blázquez E, Navas MA: Functional analysis of human glucokinase gene mutations causing MODY2: exploring the regulatory mechanisms of glucokinase activity. Diabetologia 2007;50:325-333
50. Porter JR, Shaw NJ, Barrett TG, Hattersley AT, Ellard S, Gloyn AL: Permanent neonatal diabetes in an Asian infant. J Pediatr 2005;146:131-133

51. Raimondo A, Chakera AJ, Thomsen SK, Colclough K, Barrett A, De Franco E, Chatelas A, Demirbilek H, Akcay T, Alawneh H, Flanagan SE, Van De Bunt M, Hattersley AT, Gloyn AL, Ellard S: Phenotypic severity of homozygous GCK mutations causing neonatal or childhood-onset diabetes is primarily mediated through effects on protein stability. Hum Mol Genet 2014;23:6432-6440

52. Sekine N, Cirulli V, Regazzi R, Brown LJ, Gine E, Tamarit-Rodriguez J, Girotti M, Marie S, MacDonald MJ, Wollheim CB, Rutter GA: Low lactate dehydrogenase and high mitochondrial glycerol phosphate dehydrogease in pancreatic á-cell. Potential role in nutrient sensing. JBiolChem 1994;269:4895-4902

53. van Bürck L, Blutke A, Kautz S, Rathkolb B, Klaften M, Wagner S, Kemter E, Hrabé de Angelis M, Wolf E, Aigner B, Wanke R, Herbach N: Phenotypic and pathomorphological characteristics of a novel mutant mouse model for maturity-onset diabetes of the young type 2 (MODY 2). Am J Physiol Endocrinol Metab 2010;298:E512-523

54. Basco D, Zhang Q, Salehi A, Tarasov A, Dolci W, Herrera P, Spiliotis I, Berney X, Tarussio D, Rorsman P, Thorens B: alpha-cell glucokinase suppresses glucose-regulated glucagon secretion. NatCommun 2018;9:546-03034

55. Reimann F, Gribble FM: Glucose-sensing in glucagon-like peptide-1-secreting cells. Diabetes 2002;51:2757-2763

56. Johnson D, Shepherd RM, Gill D, Gorman T, Smith DM, Dunne MJ: Glucose-dependent modulation of insulin secretion and intracellular calcium ions by GKA50, a glucokinase activator. Diabetes 2007;56:1694-1702

Figure legends

Figure 1. **Design and genomic map of the Gck^{KI} mouse allele**. **A)** The 3' *Glucokinase* (*Gck*) coding sequence comprising exon-4 to exon-10 was directly fused in frame with endogenous exon-3. This was followed by an IRES, mCardinal cDNA and termination signal plus human growth hormone (hGH) polyA. The construct is expected to produce a single bicistronic mRNA expressing Glucokinase and mCardinal from the same mRNA transcript. **B)** Wildtype *Gck* mRNA structure. **C)** Observed sequence expressed from the knock-in allele. Sanger sequencing of the *Gck* PCR product from Gck$^{KI/KI}$ islet cDNA revealed alternative splicing in which exon 2 and exon 3 are skipped. Alpha-fold predicted 3D structure of **D)** wildtype mouse glucokinase and **E)** the mis-spliced isoform. The green matrix represents the confidence in the prediction in Angstroms, with darker shades indicating greater confidence. The beta-barrel that forms part of the glucose-binding pocket and ATP binding domain (pink, D) is absent from the modelled mis-spliced isoform (E).

Figure 2. **Apparent GK protein levels in male and female pancreatic islets. A)** Western (immuno-) blot images from islets protein from wildtype, Gck$^{KI/+}$ (heterozygous) and Gck$^{KI/KI}$ (homozygous) males and females. Glucokinase was detected at ~48kDa and beta-actin at ~45kDa. **B)** Quantitative analysis of GK expression levels normalized to beta-actin across sex and genotype. Each dot represents a single animal. Unpaired one-way ANOVA with Tukey's correction. *$P \leq .05$, **$P \leq .01$, ***$P \leq .001$.

Figure 3. **Metabolic characterization of Gck$^{KI/+}$ ^{and} Gck$^{KI/KI}$ mice**. **A)** Representative images across male genotypes. **B)** Mouse weight at 8 weeks of age across sex and genotype, *n*=15 WT, 10 Het and 4 Homo. Females, *n*=13 WT, 13 Het and 5 Homo. **C)** HbA1c at 8-16w across sex and genotype. Homozygous animals exhibit a diabetic phenotype in both males and females (HbA1c% > 10). Males, *n*=7 WT, 8 Het, and 8 Homo. Females, *n*=5 WT, 6 Hets and 8 Homo. Unpaired one-way ANOVA with Tukey's correction. **D)** Intraperitoneal glucose tolerance tests (IPGTT) with 2 g/kg glucose performed at 8-16w of age for males (*n*=12 WT and 9 Hets) and females (*n*=12 WT and 13 Hets). Unpaired one-way ANOVA with Šidák's correction. **E)** Glucose excursion (area under the curve, AUC) quantifications from the male and female IPGTTs presented in (D). Unpaired one-way ANOVA with Tukey's correction. **F)** Intraperitoneal insulin tolerance test (IPTT) with 0.75 insulin units/Kg performed at 8-16w. Males, *n*=10 WT, 6 Hets. Females, *n*=7 WT, 7 Hets. Unpaired two-way ANOVA with Šidák's

correction. **G)** Glucose AUC quantifications of IPGTTs presented in (F). Unpaired one-way ANOVA with Tukey's correction. The homozygous fasting values are represented by the red triangle (*n*=3 mice) in (D) and (F). Due to the high fasting glucose, IPGTT and IPTT were not performed in homozygotes, and the fasting glucose levels are presented as a reference only. **H)** Insulin secretion from isolated islets across genotypes and sexes. * (I) Ketone body levels in fasted animals. *N*=3-5 per group. $P \leq .05$, $^{**}P \leq .01$, $^{***}P \leq .001$, $^{****}P \leq .0001$.

Figure 4. **Dorzagliatin restores glucose-induced Ca^{2+} dynamics and β-cell connectivity in $Gck^{KI/+}$ mouse islets. A)** Experimental design for *in vitro* calcium imaging in islets from 8-16w Ins1Cre:GCaMP6f$^{fl/fl}$:Gck$^{+/+}$ ("WT"), Gck$^{KI/+}$ ("Het") and Gck$^{KI/+}$ ("Homo") triple transgenic mice. Where indicated, isolated islets were treated for 1h with 10μM dorzagliatin prior to imaging. **B)** Snapshots from confocal time-lapses recordings of the individual islets at 6 Hz in 11mM glucose with or without 10μmol/L dorzagliatin across *Gck* genotypes. **C)** Normalized GCaMP6f fluorescence traces from islets shown in (B). **C)** Raster plots show the apparent Ca^{2+} signal for individual cells from islets shown in (B). **D)** Visualization of the islet functional network for each genotype, with or without dorzagliatin, from islets displayed in (B). **E)** Calcium AUC quantification across genotypes in control and dorzagliatin treated islets. **F)** Connectivity quantifications across genotypes in control and dorzagliatin treatment groups. Unpaired one-way ANOVA with Tukey's correction. $^{*}P \leq .05$, $^{**}P \leq .01$, $^{***}P \leq .001$, $^{****}P \leq .0001$. For 11 mmol/L glucose-only treatment, *n*=5 WT mice (9 islets), n=8 heterozygotes (14 islets) and n=4 homozygotes (7 islets). For dorzagliatin treatment, *n*=4 WT (6 islets), *n*=5 heterozygotes (13 islets) and *n*=4 homozygotes (11 islets). Each dot represents an individual islet. The numbers 1, 2, and 3 in the snapshots displayed in (B) indicate the time points corresponding to the fluorescence traces showed in (C). Scale bar, 25 μm.

Figure 5. **Impact of dorzagliatin and exendin-4 on glucose tolerance across genotypes and sexes. A-B)** Intraperitoneal glucose tolerance test (IPGTT) with 2 g/kg glucose performed in animals of 8-16w of age for males and females after injection of glucose only or glucose in combination with dorzagliatin (1mg/kg), exendin-4 (1nmol/kg) or dorzagliatin (1mg/kg) + exendin-4 (1nmol/kg) in WT (Gck$^{+/+}$) or heterozygous (Gck$^{KI/+}$) animals. The first panel in grey corresponds to the same data shown in Fig. 3D. Unpaired two-way ANOVA with Šidák's correction. **C-D)** Glucose AUC quantifications of each IPGTT treatment from male and female mice presented in (A) and (B). Males, *n*=4

WT, 7 Hets for each treatment; Females, *n*=5 WT, 10 Hets for each treatment. Unpaired one-way ANOVA with Tukey's correction. **E)** Glucose AUC quantifications of each IPGTT treatment from pooled male and female mice presented in (A) and (B), and homozygous ($Gck^{KI/KI}$) mice treated with PBS alone, or PBS and dorzagliatin (1mg/kg), exendin-4 (1nmol/kg) or dorzagliatin (1mg/kg) + exendin-4 (1nmol/kg). Males: *n*=4 WT, *n*=4 Hets, *n*=2 Homo for each treatment, *n*=1-Homo (PBS); Females *n*=7 WT, *n*=7 Hets, *n*=5 Homo for each treatment, *n*=4 Homo (PBS). Unpaired one-way ANOVA with Tukey's correction. *P ≤ .05, **P ≤ .01, ***P ≤ .001, ****P ≤ .0001 **P* ≤ .05, ***P* ≤ .01, ****P* ≤ .001, *****P* ≤ .0001.

Figure 6. **Impact of dorzagliatin and incretin on glucose-stimulated insulin secretion *in vitro*. A-B)** Insulin secretion *in vitro* for male (A) and female (B) at low (3mmol/L) and high (17mmol/L) glucose concentrations. **C)** Stimulation index, calculated as the ratio of insulin secreted at 17 mmol/L glucose to that at 3 mmol/L glucose, from pooled islets of both sexes across genotypes. One-way ANOVA of Brown-Forsythe. Mean ± SD. *P<0.05, **P<0.01, ***P<0.001, ****P<0.0001.

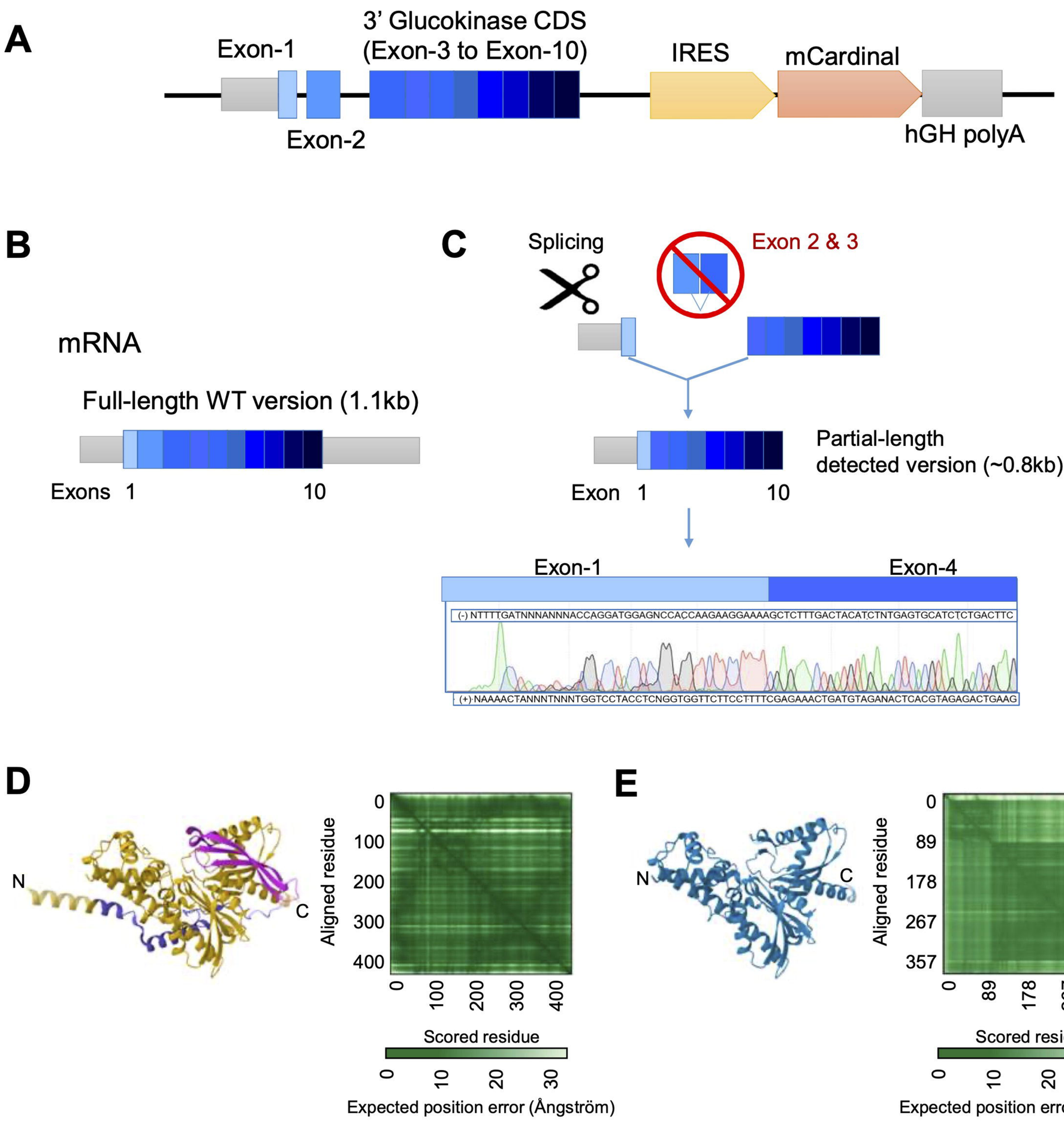

Figure 1

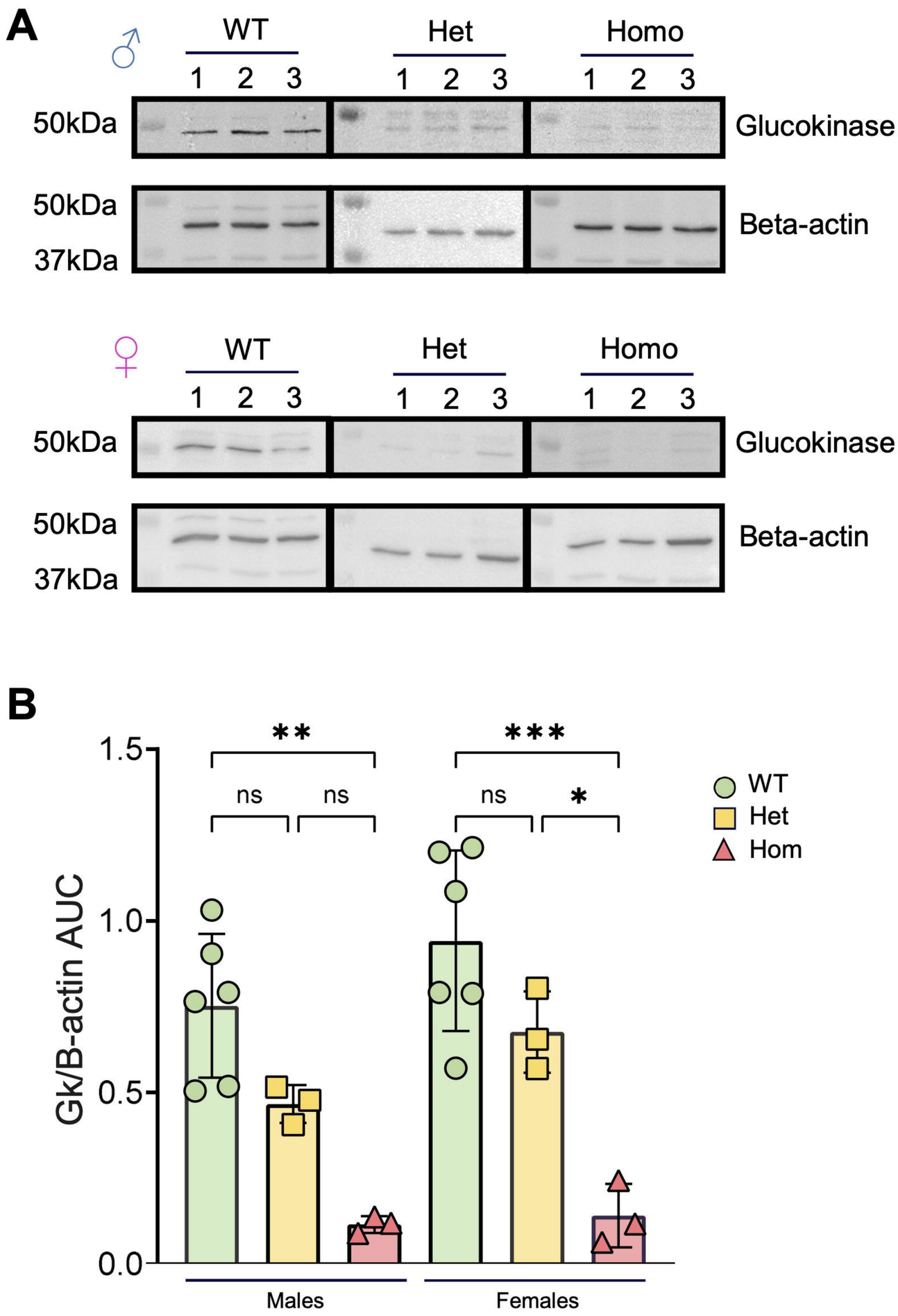

Figure 2

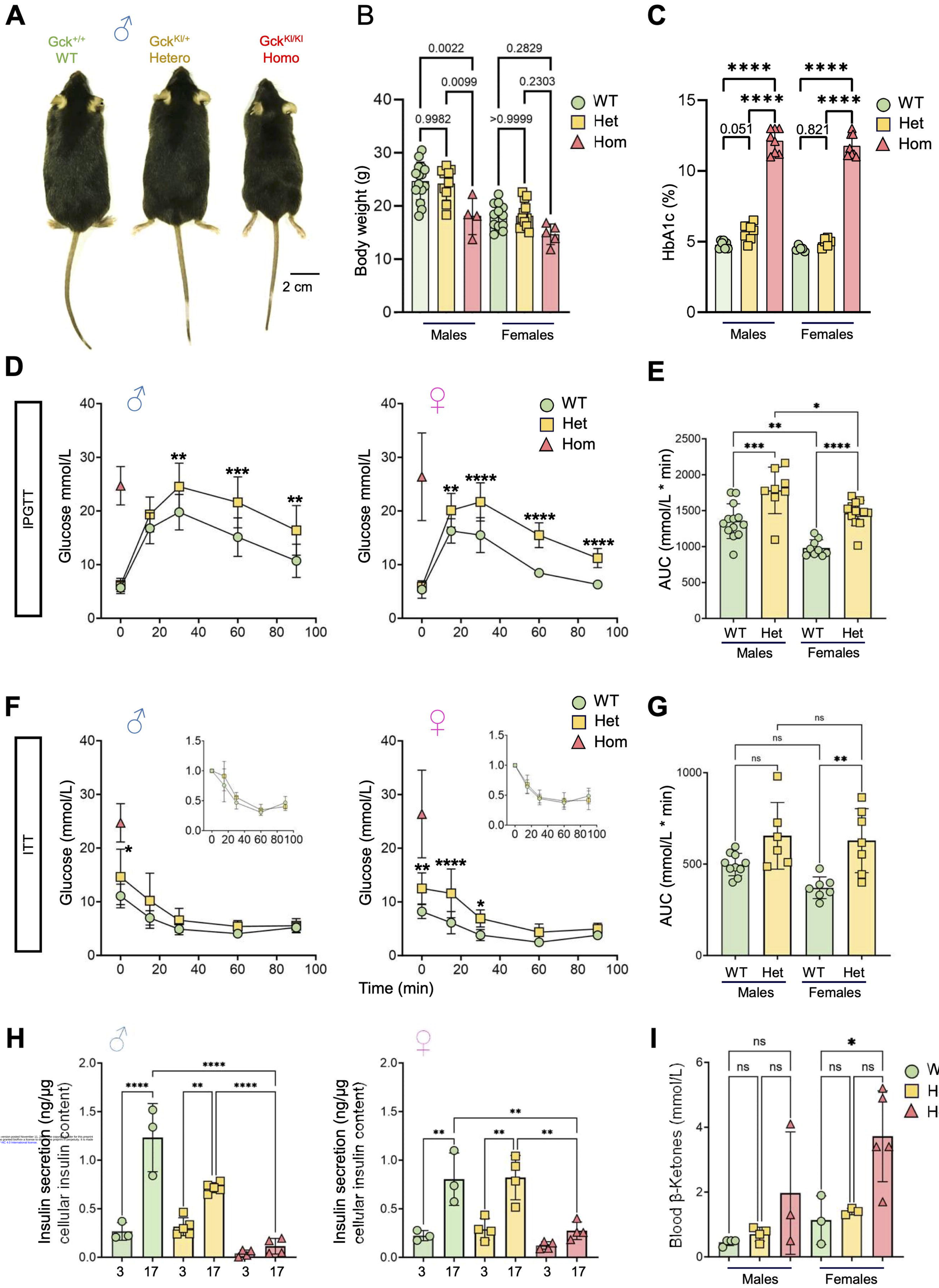

Figure 3

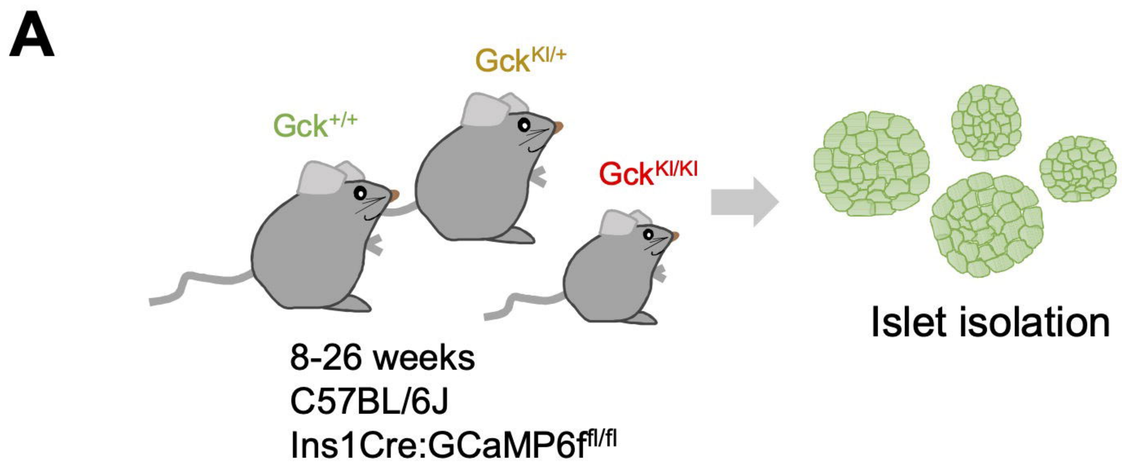

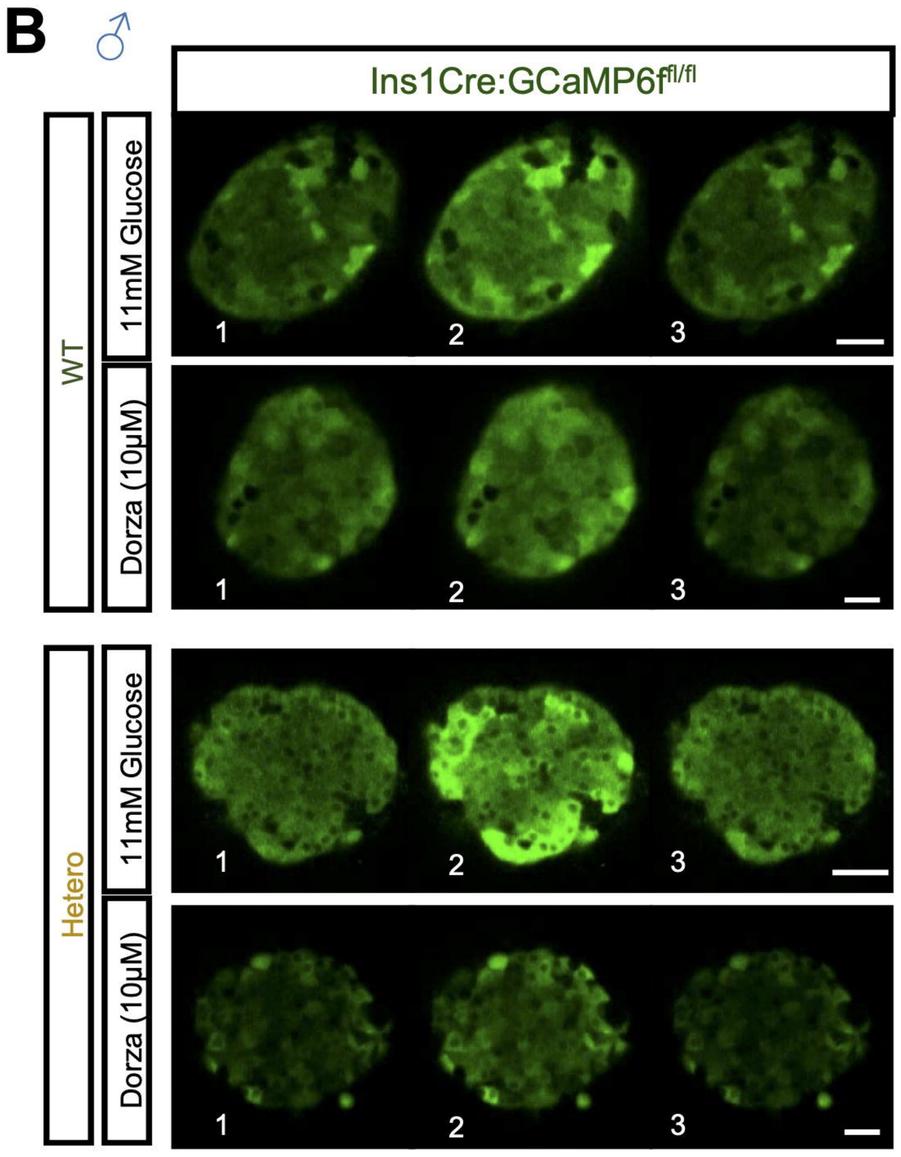

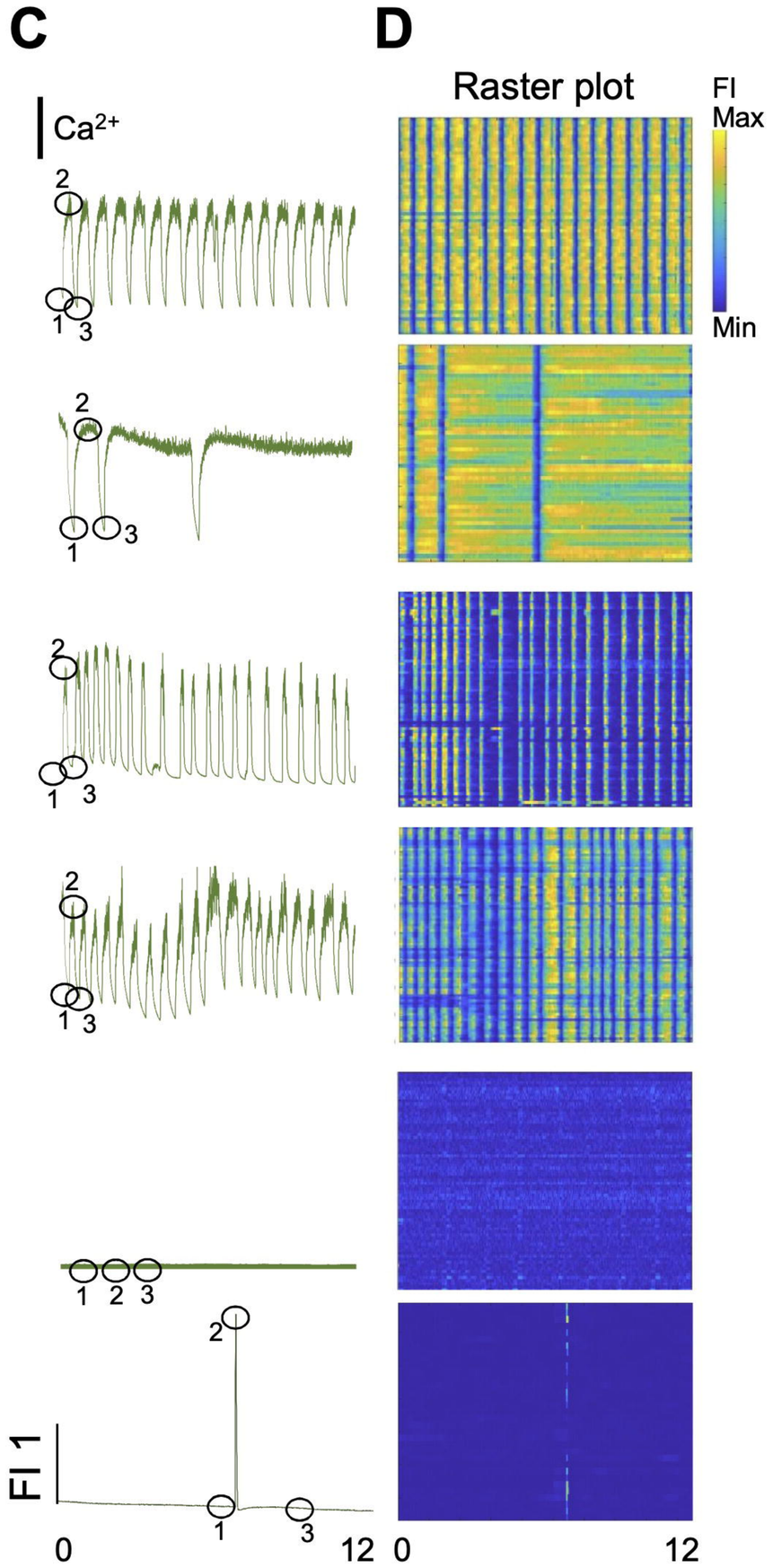

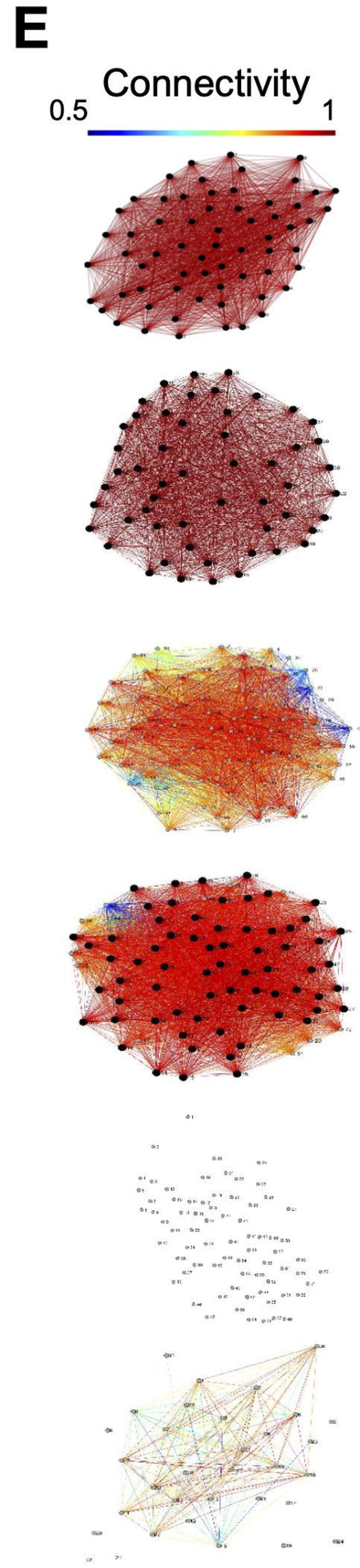

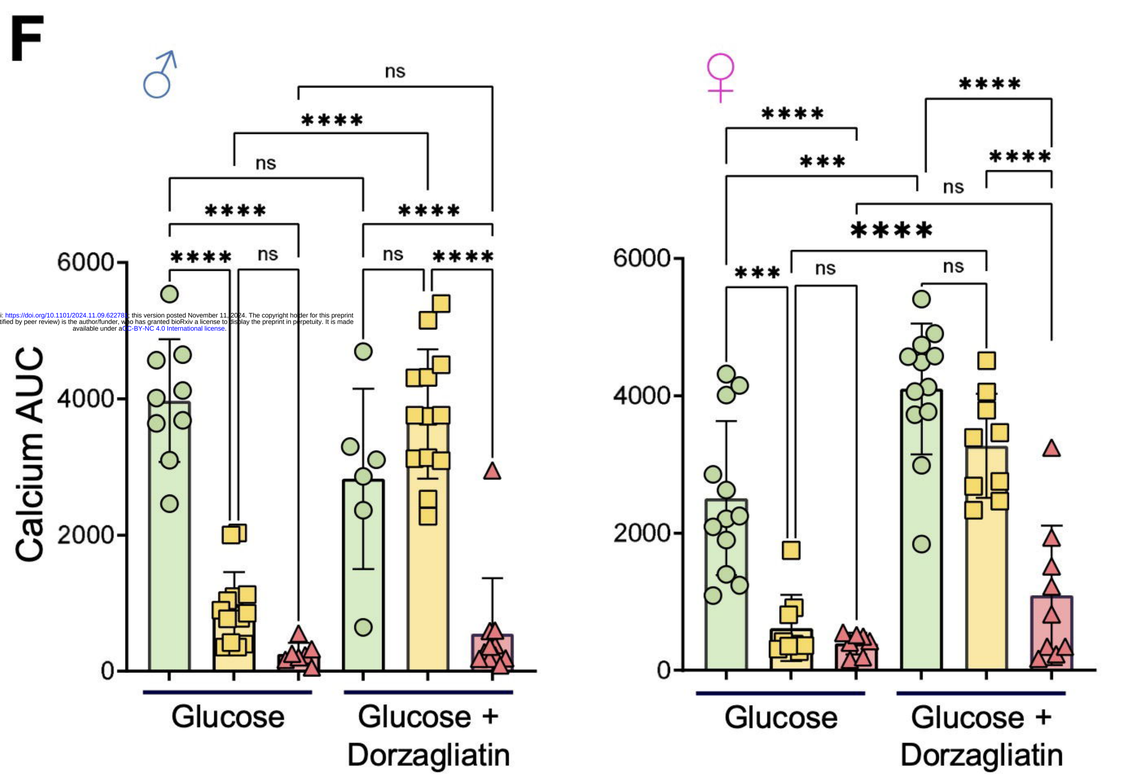

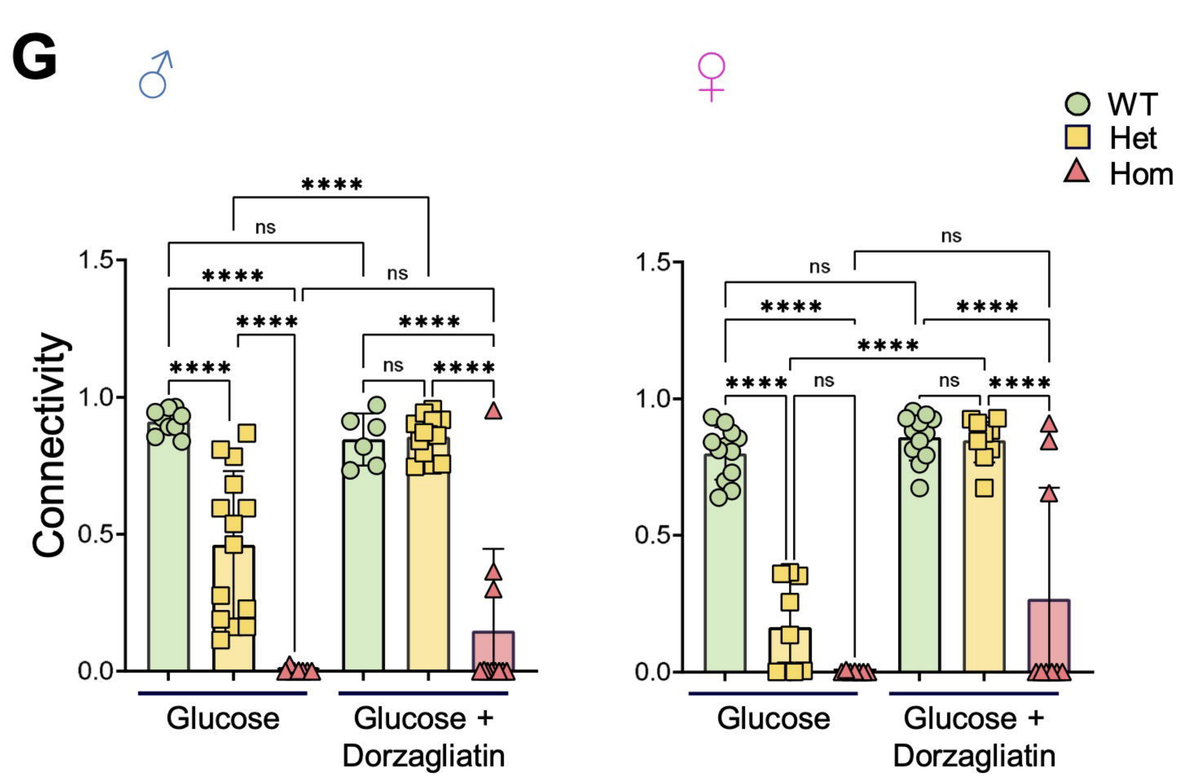

Figure 4

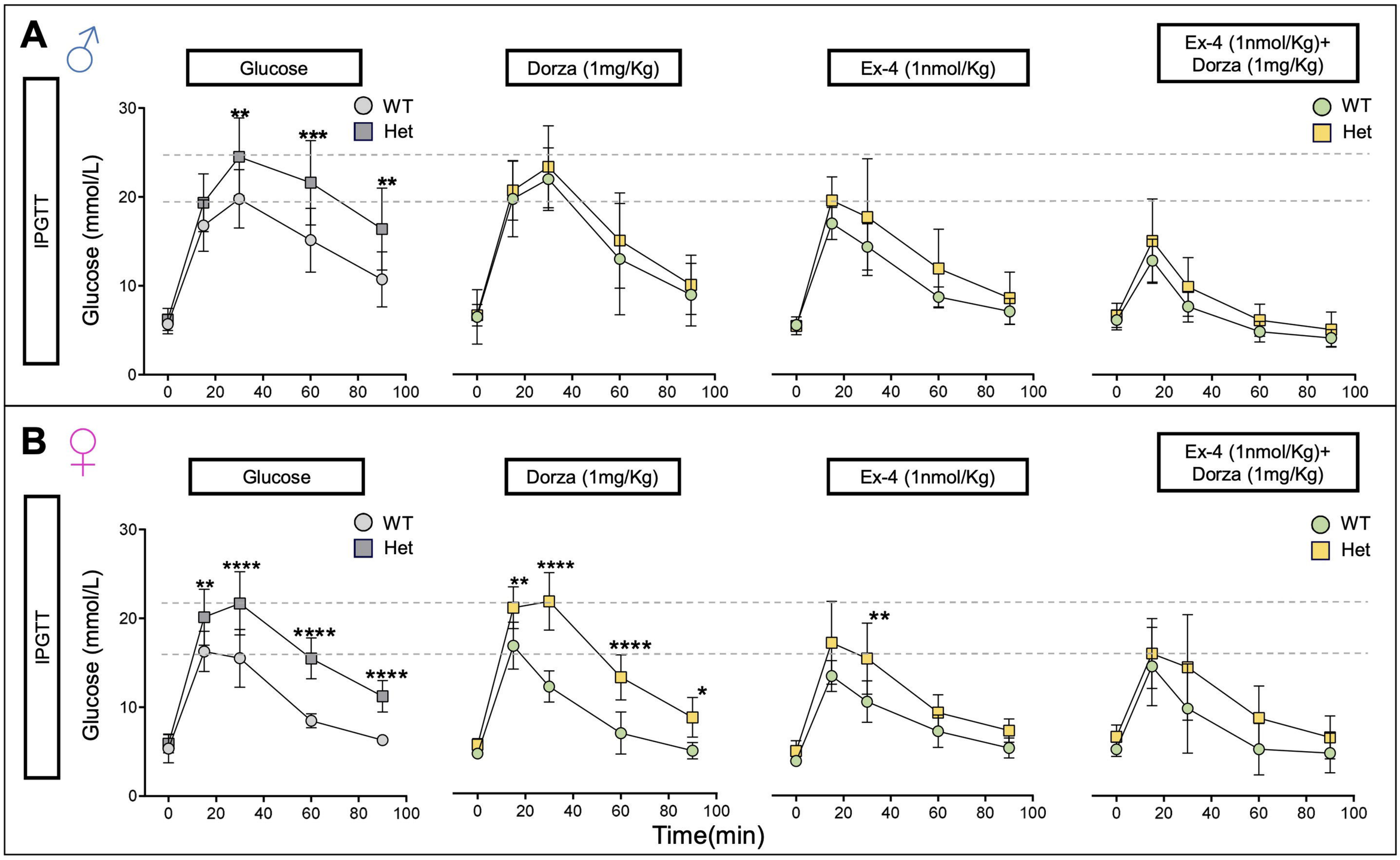

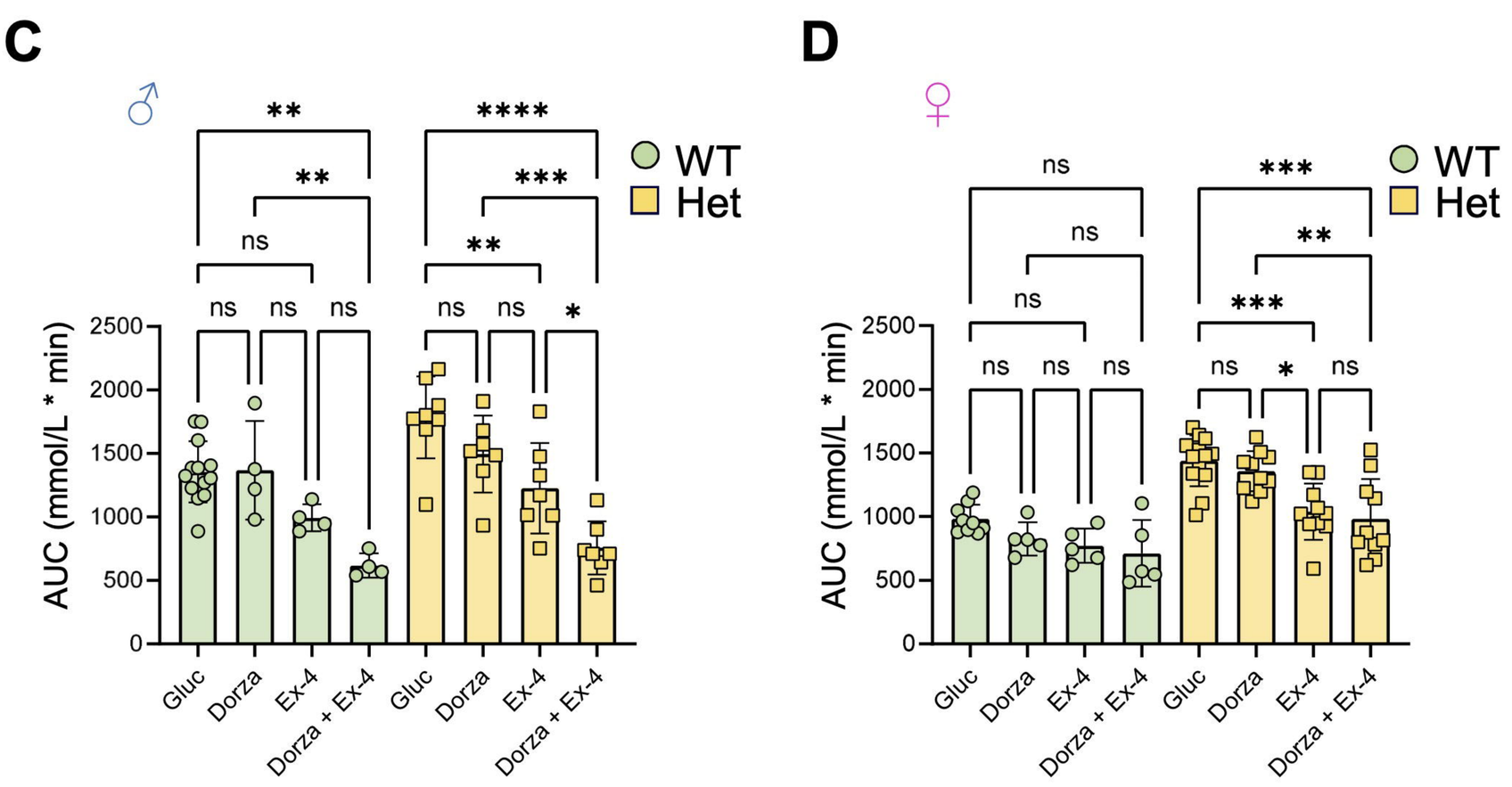

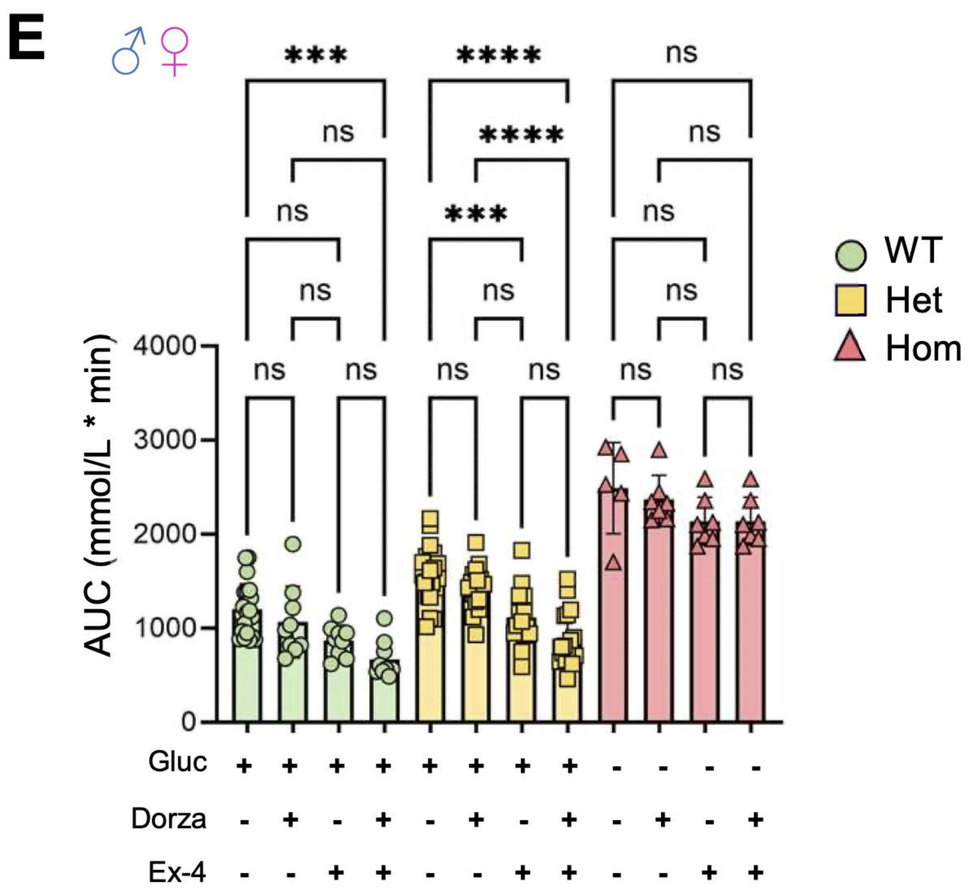

Figure 5

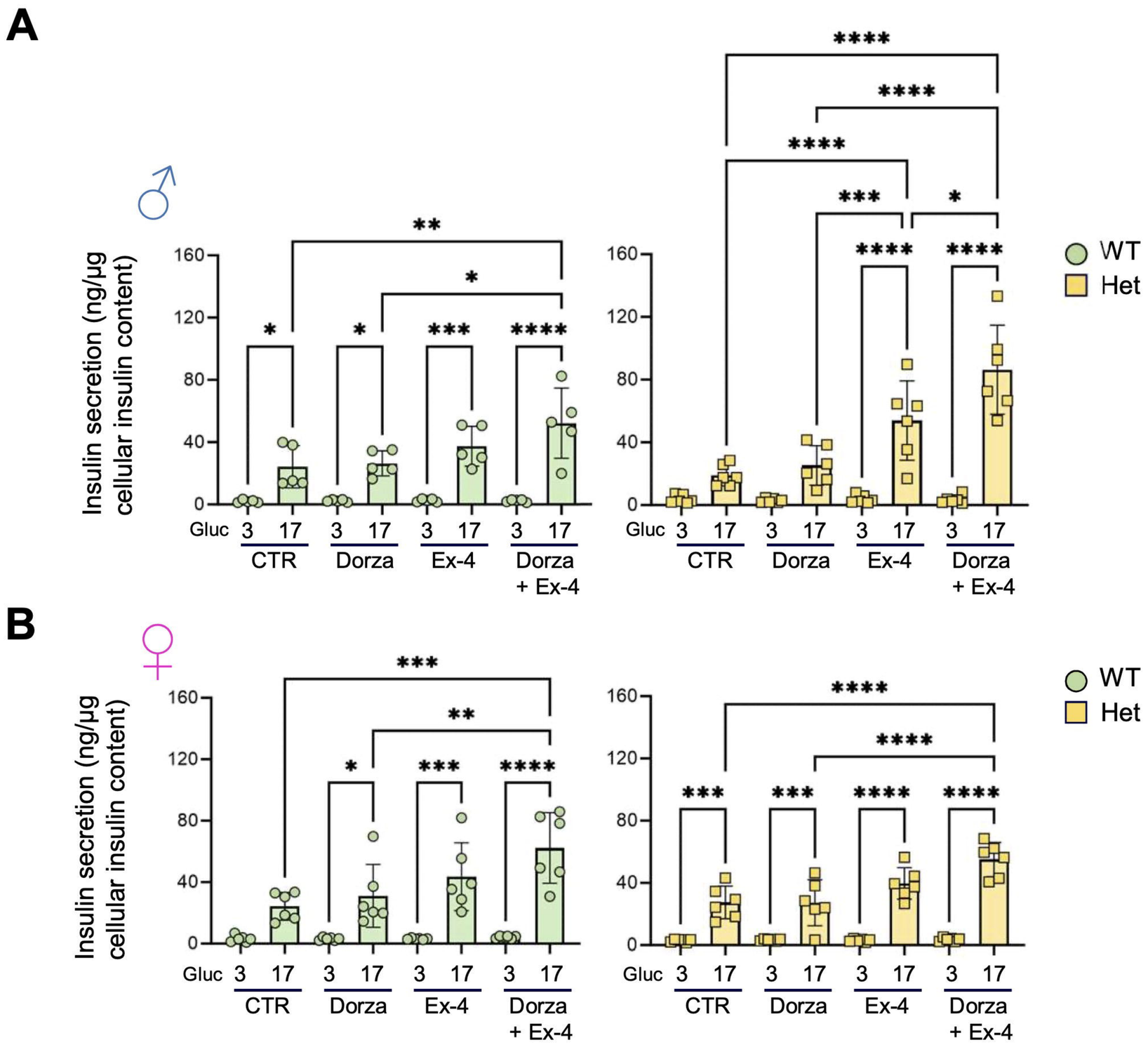

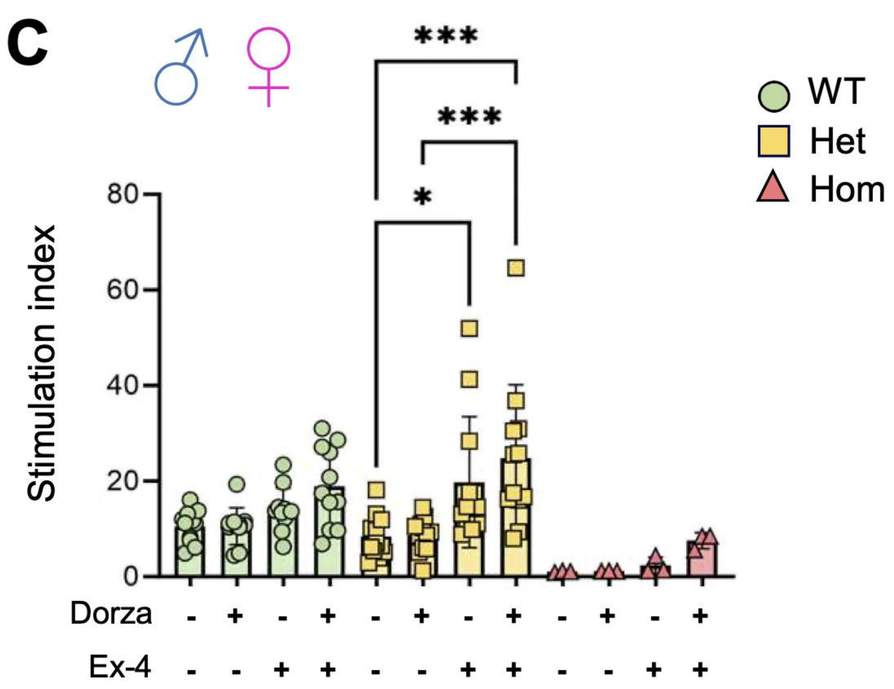

Figure 6